

1

2 TITLE

3 A simple microbiome in esophagus and gills of the European common cuttlefish, *Sepia*

4 *officinalis*

5

6 RUNNING TITLE

7 A simple microbiome in cuttlefish esophagus and gills

8

9 Holly L. Lutz^{a,b,c,†,*}, S. Tabita Ramírez-Puebla^{d,†}, Lisa Abbo^d, Cathleen Schlundt^d,

10 Alexandra K. Sjaarda^a, Amber Durand^d, Roger T. Hanlon^d, Jack A. Gilbert^{a,b,c,*}, Jessica

11 L. Mark Welch^{d,*}

12

13 ^aMicrobiome Center, University of Chicago, Chicago, IL 60637

14 ^bDepartment of Surgery, University of Chicago, Chicago, IL 60637

15 ^cIntegrative Research Center, Field Museum of Natural History, Chicago, IL 60605

16 ^dMarine Biological Laboratory, Woods Hole, MA 02543

17

18 [†] co-first authors, contributed equally to this work

19 ^{*}to whom correspondence should be addressed. Email address: hlutz@fieldmuseum.org

20 or jmarkwelch@mbl.edu

21

22

23

24 ABSTRACT

25

26 The European common cuttlefish, *Sepia officinalis*, is used extensively in biological and
27 biomedical research yet its microbiome remains poorly characterized. We analyzed the
28 microbiota of the digestive tract, gills, and skin in mariculture-raised *S. officinalis* using a
29 combination of 16s rRNA amplicon sequencing and fluorescence spectral
30 imaging. Sequencing revealed a highly simplified microbiota consisting largely of two
31 single bacterial amplicon sequence variants (ASVs) of Vibrionaceae and
32 Piscirickettsiaceae. The esophagus was dominated by a single ASV of the
33 genus *Vibrio*. Imaging revealed a striking organization of bacteria distributed in a discrete
34 layer that lines the esophagus. Imaging with specific probes confirmed the identity of
35 these bacteria as Vibrionaceae. This *Vibrio* was also abundant in the microbiota of the
36 stomach, cecum, and intestine, but occurred at lower density and in the lumen rather than
37 in a discrete layer; it was present in only trace proportions in tank water and in the
38 microbiome of shrimp that were used as feed for the
39 cuttlefish. These *Vibrio* were resilient to treatment of animals with the commonly-used
40 antibiotic, enrofloxacin. The gills were colonized by a single ASV in the family
41 Piscirickettsiaceae, which imaging visualized as small clusters of cells. We conclude that
42 bacteria belonging to the Gammaproteobacteria, especially Vibrionaceae, are the major
43 symbionts of the cuttlefish *Sepia officinalis* cultured from eggs in captivity, and that the
44 esophagus and gills are major colonization sites.

45

46

47 IMPORTANCE

48

49 Microbes can play critical roles in the physiology of their animal hosts, as evidenced in
50 cephalopods by the role of *Vibrio (Aliivibrio) fischeri* in the light organ of the bobtail
51 squid and the role of Alpha- and Gammaproteobacteria in the reproductive system and
52 egg defense in a variety of cephalopods. We sampled the cuttlefish microbiome
53 throughout the digestive tract, gills, and skin and found dense colonization of an
54 unexpected site, the esophagus, by a microbe of the genus *Vibrio*, as well as colonization
55 of gills by Piscirickettsiaceae. We found these associations to be resilient to the treatment
56 of animals with a common antibiotic, enrofloxacin. This finding expands the range of
57 organisms and body sites known to be associated with *Vibrio* and is of potential
58 significance for understanding host-symbiont associations as well as for understanding
59 and maintaining the health of cephalopods in mariculture.

60

61 KEYWORDS:

62 microbiome, fluorescence *in situ* hybridization, *Photobacterium*, Vibrionaceae,
63 Piscirickettsiaceae

64

65 1. INTRODUCTION

66

67 Symbiotic associations between invertebrates and bacteria are common. Among
68 cephalopods, the most intensely studied association is the colonization of the light organ
69 of the bobtail squid *Euprymna scolopes* by the bioluminescent bacterium *Vibrio*

70 (*Aliivibrio*) *fischeri* in a highly specific symbiosis (1). A more diverse but still
71 characteristic set of bacteria colonize the accessory nidamental gland from which they are
72 secreted into the egg jelly coat and likely protect the eggs from fungal and bacterial
73 attack (2). The accessory nidamental gland and egg cases of the squid *Doryteuthis*
74 (*Loligo*) *pealeii* and the Chilean octopus (*Octopus mimus*) have also been reported to
75 contain Alphaproteobacteria and Gammaproteobacteria (3, 4). These associations indicate
76 that bacteria can play a critical role in the physiology of cephalopods.

77 *Sepia officinalis*, the European common cuttlefish (hereafter cuttlefish), is used
78 extensively in biological and biomedical research (5-7) and is a model organism for the
79 study of rapid adaptive camouflage (8-11). Cuttlefish are also widely represented among
80 zoos and aquaria, and play an important role in educating the public about cephalopod
81 biology and life history (12). Little is known about the association of bacterial symbionts
82 with cuttlefish, and whether such associations may play a role in the health or behavior of
83 these animals. Because cuttlefish behavior is well-studied and there exist standardized
84 methods for documenting multiple behaviors (8), we hypothesized that these animals may
85 provide a unique opportunity to study microbes and the gut-brain axis – the effect of gut
86 microbiota on behavior (13) – in an invertebrate system. Understanding the importance,
87 or lack thereof, of the cuttlefish microbiome will not only shed light on the basic biology
88 of this model organism, but will also have practical implications for future husbandry
89 practices and research design.

90 Using a combination of 16s rRNA amplicon sequencing and fluorescence *in situ*
91 hybridization (FISH), we characterized the gastrointestinal, gill, and skin microbiota of
92 the common cuttlefish in wild-bred, captive-raised animals (5) housed at the Marine

93 Biological Laboratory (Woods Hole, MA). In addition to baseline microbiome
94 characterization, we examined the extent to which cuttlefish microbiota were responsive
95 to antibiotic treatment, and conducted behavioral experiments to assess possible effects of
96 the microbiota on two well-studied behaviors: camouflage and feeding.

97

98 2. RESULTS

99

100 2. 1 Two taxa dominate the *S. officinalis* microbiome.

101

102 This study comprised two time points – the first (20-21 June 2017) in which three
103 healthy adult *S. officinalis* from the mariculture laboratory at Marine Biological
104 Laboratory (Woods Hole, MA) were sampled, and the second (25 September -10 October
105 2017) in which antibiotic trials were conducted on 24 healthy adult *S. officinalis* (16
106 treatment individuals, 8 control individuals). 16s rRNA amplicon sequencing of the
107 gastrointestinal tract, gills, and skin of *S. officinalis* revealed a highly simplified
108 microbiota dominated by bacterial amplicon sequence variants (ASVs) in the
109 Vibrionaceae and Piscirickettsiaceae. These results were consistent across both the pilot
110 study and in the experimental study.

111 In particular, results showed a consistent and highly simplified microbiota in the
112 esophagus (Fig. 1; Table 1). A single ASV in the genus *Vibrio* made up the majority of
113 the sequence data from the esophagus of the three pilot investigation animals (mean
114 $92.4\% \pm 9.8$). This ASV was also detected in high abundance among experimental
115 animals four months later, in control animals (mean $99.5\% \pm 1.2$) and treatment animals

116 (mean $94.4\% \pm 10.8$). Thus, this ASV represents a dominant constituent of the esophagus
117 microbiota stably over the two time points of this study. We note that another ASV of the
118 related genus *Photobacterium* (Vibrionaceae) was present in the esophagus community in
119 the pilot investigation animals (mean $6.8\% \pm 10$). Combined, the two Vibrionaceae ASVs
120 in these pilot animals constituted 99.2% of the esophagus community.

121 The major *Vibrio* ASV was also a major constituent of downstream sites in the
122 digestive tract, and differed significantly between control and treatment groups for the
123 most distal digestive organs (cecum and intestine) (Fig. 1; Table 1). The remainder of the
124 sequence data from the digestive tract consisted of an assortment of taxa that varied
125 between individuals or between the two time points of the study and thus suggest
126 transient rather than stable microbial colonization. We thus consider the *Vibrio* ASV to
127 be the dominant microbe of the lower digestive tract in these cuttlefish, although not in
128 the same density and discrete layering as the esophagus (see 2.3).

129 Samples from gills were dominated by a single highly abundant ASV, classified
130 as family Piscirickettsiaceae and making up an average $96.9\% \pm 2.5$ in the gills of control
131 animals, and $82.4\% \pm 1.9$ in treated animals. In samples from other body sites this ASV
132 was detected only sporadically and at low abundance (mean 0.2%, range 0 to 5.8%) (Fig.
133 1).

134

135 2.2 Effect of antibiotic treatment on *S. officinalis* microbiome composition and behavior

136

137 Analysis of behavioral data found no differences in the expression of disruptive
138 camouflage behavior between cuttlefish before and after antibiotic treatment ($p = 0.7$,

139 paired t-test), or between treatment and control groups after antibiotic treatment ($p =$
140 0.62, t-test). Similarly, no differences in predation behavior (*i.e.* hunting live shrimp)
141 were observed between cuttlefish before and after antibiotic treatment ($p = 0.65$, paired t-
142 test), or between treatment and control groups after antibiotic treatment ($p = 0.58$, t-test).
143 Treatment of *S. officinalis* with the antibiotic enrofloxacin therefore had no discernable
144 effects on camouflage or feeding behaviors, and resulted in only modest changes to the
145 microbiome. Between organs (gills, esophagus, stomach, cecum, and intestine) of
146 treatment and control groups, we observed a small but significant difference in Shannon
147 diversity ($p = 1.55e-7$, t-test) but saw no difference in observed ASV richness ($p = 0.46$,
148 t-test). We also found experimental group (treatment vs control) to be a significant
149 predictor of weighted UniFrac dissimilarity ($p < 0.01$, $R^2 = 0.042$, ADONIS),
150 unweighted UniFrac dissimilarity ($p < 0.01$, $R^2 = 0.021$, ADONIS), and Bray-Curtis
151 dissimilarity ($p < 0.01$, $R^2 = 0.040$, ADONIS).

152 The single *Vibrio* ASV maintained dominance in the digestive tract and did not
153 differ significantly in relative abundance within the esophagus or stomach of treatment
154 and control groups ($p > 0.09$, t-test). In the more distal organs of the digestive tract,
155 however, the relative abundance of the major *Vibrio* ASV showed a dramatic and
156 significant drop in mean relative abundance. In the cecum, this sequence made up an
157 average $43.7\% \pm 23.4$ of the community in control individuals and only $6.4\% \pm 8.7$ in
158 antibiotic-treated individuals ($p = 0.002$, t-test); in intestine the average from control
159 animals was $56.8\% \pm 15.8$, and only $5.5\% \pm 5.9$ in antibiotic-treated animals ($p = 1.99e-$
160 05, t-test) (Table 1). A single Piscirickettsiaceae ASV maintained dominance in the gills

161 of treated cuttlefish (Fig. 1; Table 1), although its relative abundance did differ
162 significantly between treatment and control groups ($p = 0.01$, t-test) (Table 1).

163

164 2.3 Imaging shows high microbial abundance and spatial structure in cuttlefish esophagus
165 and lower abundance and scattered distribution elsewhere in the digestive tract.

166

167 Fluorescence *in situ* hybridization (FISH) revealed a striking organization of
168 bacteria distributed in a layer lining the interior of the convoluted esophagus of cuttlefish
169 (Fig. 3). Hybridization with the near-universal Eub338 probe showed bacteria in high
170 density in a layer ~20-40 μm thick at the border between host tissue and lumen. Staining
171 with fluorophore-conjugated wheat germ agglutinin revealed a mucus layer that covered
172 the epithelium and generally enclosed the bacteria. To verify the identity of these bacteria
173 we employed a nested probe set including Eub338 as well as probes for
174 Alphaproteobacteria, Gammaproteobacteria, and one of two probes we designed
175 specifically for Vibrionaceae (Vib1749 and Vib2300, Table 2). Bacterial cells imaged in
176 the esophagus showed signal from all probes expected to hybridize with Vibrionaceae,
177 suggesting that the bacteria observed in this organ are a near-monoculture of this taxon
178 (Fig. 4B-D). The probe targeted to Alphaproteobacteria was included in the FISH as a
179 negative control and, as expected, did not hybridize with the cells (Fig. 4E). As an
180 additional control to detect non-specific binding of probes, we performed an independent
181 FISH with a set of probes labeled with the same fluorophores as the experimental probe
182 set, but conjugated to oligonucleotides not expected to hybridize with the cuttlefish
183 microbiota (Table 2). No signal from this non-target probe set was detected (Fig. 4F,G)

184 supporting the interpretation that the signal observed in the esophagus results from a
185 specific interaction of the Vibrionaceae-targeted oligonucleotides with the visualized
186 bacteria.

187 In other parts of the digestive tract we observed a sparser distribution of bacteria
188 without obvious spatial organization. Bacteria in the intestine were present not in a layer
189 but scattered throughout the lumen and mixed with the luminal contents (Fig. 5).

190 Similarly, in cecum bacteria were observed in low abundance in the lumen (Fig. 6). FISH
191 was also applied to the stomach, posterior salivary gland (poison gland) and duct of the
192 salivary gland, but no bacteria were detected (not shown).

193 Fluorescence *in situ* hybridization to cross-sections of the gills revealed clusters
194 of bacteria (Figure 7). Gill samples were embedded in methacrylate resin and sectioned
195 to 5 µm thickness, and FISH applied to the sections with universal probes (Fig. 7) and
196 probes for Alpha- and Gammaproteobacteria (Fig. 7). Results showed hybridization of
197 probes for gamma but not alpha proteobacteria, consistent with the identification of the
198 clusters of gill bacteria as members of the gamma proteobacteria family
199 Piscirickettsiaceae.

200

201 3. DISCUSSION

202

203 We sampled the cuttlefish microbiome of the digestive tract, gills, and skin and
204 found dense colonization of an unexpected site, the esophagus, by a microbe of the genus
205 *Vibrio*. Both imaging and ribosomal RNA gene sequencing showed a near-monoculture
206 of *Vibrionaceae* in the esophagus, with imaging showing dense colonization of the

207 interior lining of the esophagus with a single morphotype that hybridized to probes
208 targeting *Vibrionaceae*. In the remainder of the digestive tract, both imaging and
209 sequencing indicated a less consistent microbiota. Sequencing showed lower relative
210 abundance of the dominant *Vibrio* ASV. Imaging showed sparse and sporadic
211 colonization in the stomach, intestine, and cecum, with scattered cells in the lumen and
212 no clear colonization of the epithelium. In light of the imaging results, we interpret the
213 sequencing results as consistent with a higher colonization density in the esophagus and a
214 lower density in the distal gut. In the esophagus, the dominant *Vibrio* ASV appears to be
215 resilient to antibiotic treatment, with no significant difference in relative abundance
216 observed between groups. Moving along the digestive tract towards the distal end,
217 however, we observed striking and significant differences in the *Vibrio* relative
218 abundance between control and treatment groups. This may be due, in part, to the fact
219 that antibiotics were administered via injection into the cuttlefish food source, grass
220 shrimp, which would contain the antibiotic until broken down in the cecum and intestine
221 of the cuttlefish, thereby shielding the esophagus and stomach from coming into contact
222 with the full antibiotic dose. Alternatively, the esophagus microbiota may have formed a
223 biofilm in which the microbes were shielded from the effects of the antibiotic.

224 Diverse associations with *Vibrio* and the Vibrionaceae are known from
225 cephalopods. Among the most extensively investigated is the mutualistic association of
226 the bioluminescent *Vibrio (Aliivibrio) fischeri* with the light organ of the bobtail squid
227 *Euprymna scolopes* (1, 14). Other well-known symbioses include the colonization of the
228 cephalopod accessory nidamental gland with Alpha- and Gammaproteobacteria, which
229 enables the host to secrete a layer of bacteria into the protective coating of the egg

230 capsule (3, 15-19). Thus, colonization by Gammaproteobacteria and specifically by
231 Vibrionaceae is common in cephalopods, yet dense colonization of the digestive tract,
232 and particularly the esophagus, was unexpected.

233 Bacteria from genus *Vibrio* and the related Vibrionaceae genus *Photobacterium*
234 are frequent colonizers of the digestive tracts of marine fishes (20, 21) and are prominent
235 in the microbiota of *Octopus vulgaris* paralarvae (22). Vibrionaceae have been reported
236 to produce chitinases, proteases, amylase, and lipase (21), suggesting the possibility that
237 colonization of the digestive tract by the Vibrionaceae serves to aid in host digestion (21).
238 If the *Vibrio* and *Photobacterium* ASVs serve this function, their localization in high
239 density in the esophagus, near the beginning of the digestive tract, may serve to seed the
240 distal gut; colonization of the lining of the esophagus may provide a reservoir that
241 permits the microbes to avoid washout from the gut by continually re-populating the
242 lumen of downstream gut chambers.

243 An alternative hypothesis is that the colonization of the esophagus, and the rest of
244 the gut, is pathogenic or opportunistic. Various *Vibrio* species are known pathogens of
245 cephalopods, causing skin lesions and sometimes mortality in squids and octopuses (23-
246 25). The genus *Vibrio* includes representatives that are pathogenic to corals (*V.*
247 *coralliilyticus*), fish (*V. salmonicida*), diverse marine organisms (*V. harveyi*) and humans
248 (*V. alginolyticus*, *V. cholerae*, *V. parahaemolyticus*, and *V. vulnificus* (26, 27). Likewise,
249 the genus *Photobacterium* contains pathogenic as well as commensal representatives
250 (28). A previous study of the microbiota of *Octopus vulgaris* paralarvae found that
251 recently hatched paralarvae had a high-diversity microbiome that changed, in captivity, to
252 a lower-diversity microbiome with abundant Vibrionaceae (22). Whether the

253 Vibrionaceae are an integral part of cuttlefish physiology or whether they represent
254 opportunistic colonists of these laboratory-reared organisms is an interesting question for
255 future research.

256 Our sequence data from gills was dominated by a single ASV classified as
257 Piscirickettsiaceae that was in low abundance at other body sites. The Piscirickettsiaceae
258 are a family within the Gammaproteobacteria (29) that includes the salmon pathogen *P.*
259 *salmonis*. Rickettsia-like organisms have been described from the gills of clams and
260 oysters (30, 31) as well as associated with the copepod *Calanus finmarchicus* (32). In
261 recent years Piscirickettsiaceae have been identified in high-throughput sequencing
262 datasets from seawater and sediment as a taxon that may be involved in biodegradation of
263 oil and other compounds (33-39). Whether taxa in this family colonize the gills of
264 cuttlefish and other organisms as symbionts or as opportunistic pathogens is, again, a
265 subject for future investigation. Finally, studies of wild *S. officinalis* microbiota will be
266 informative for understanding natural host-symbiont associations under natural
267 conditions, as compared to the mariculture-reared animals in the present study. *S.*
268 *officinalis* in the eastern Atlantic and Mediterranean are known to prey on small marine
269 fishes and crabs, as compared to the grass shrimp (*Palaemonetes*) prey used in our study.
270 It remains to be seen whether such differences in diet and natural variation in
271 environmental conditions influence the association of microbial symbionts with *S.*
272 *officinalis* in the wild.

273

274 4. MATERIALS AND METHODS

275

276 4. 1 Behavioral experiment

277

278 We included 24 cuttlefish (16 test, 8 control) in an experiment designed to test the
279 effect of the antibiotic enrofloxacin on cuttlefish behavior and the composition of the
280 cuttlefish microbiome. Experimental animals were held in three separate water tables, all
281 connected to the same open-filtration system fed by filtered seawater. Within each water
282 table, animals were isolated into individual holding pens via plastic panels. Control and
283 test animals were kept in separate water tables. The experimental period lasted for 21
284 days (25 Sep – 15 Oct 2017). The treatment consisted of administering antibiotic to
285 treatment animals via injection into the food source (grass shrimp, *Palaemonetes spp.*),
286 which were then fed to the animals. The shrimp were injected with enrofloxacin (Baytril[®];
287 22.7 mg/mL, Bayer HealthCare LLC, Shawnee Mission, KS, USA) using a 0.5 cc, U-100
288 insulin syringe with an attached 28 g x 1/2” needle (Covidien LLC, Mansfield, MA,
289 USA). The antibiotic dosage was 10 mg/kg rounded up to the nearest hundredth mL. The
290 antibiotic was injected into the coelomic cavity of the shrimp which were then
291 immediately fed to the cuttlefish once daily for 14 days. Behavioral assays were run for 7
292 days prior to antibiotic treatment, followed by a 7-day antibiotic treatment period, after
293 which behavioral assays were repeated as antibiotics continued to be administered for 7
294 additional days.

295 We conducted two behavioral assays. The first assay was designed to elicit high
296 contrast disruptive camouflage patterns in the cuttlefish, as described in Hanlon 1988 (8,
297 9, 11). Animals were placed in a holding pen (connected to the same filtered seawater
298 system as the animals’ home water tables) comprising a base and a circular wall

299 exhibiting high contrast black and white checkered squares (8, 9, 11, 40). The holding
300 pen was covered in black fabric and contained a camera stationed directly above the
301 animals, so that behavior could be documented without disturbing the animal. Each trial
302 began once the animal had ceased swimming and had settled in a stationary position.
303 Each animal was subjected to two trials per day for four days, for a total of 6 trials per
304 animal, with at least 4 hours in between any individual's trial period. This protocol was
305 followed before antibiotic treatment (25-28 September 2017) and ten days later following
306 antibiotic treatment (9-12 October). For disruptive camouflage experiments, animals
307 were assigned discrete scores based on 11 chromatic elements (8, 41). Scores for
308 individual elements were combined for one cumulative score per trial. These scores were
309 then averaged for each individual across trials conducted before and after antibiotic
310 treatment. Scores were compared between treatment and control groups after antibiotic
311 administration, and within treatment and control groups before and after antibiotic
312 administration (e.g. treatment before vs. treatment after antibiotic administration) using
313 the Student's t-test.

314 In the second experiment, referred to as the feeding experiment, the same holding
315 pen and recording setup were used, but with the high-contrast background exchanged for
316 a neutral background (as shown in Fig. 1). The trial began once the animal settled
317 (stopped swimming), at which point a clear glass jar containing 5 healthy and active grass
318 shrimp was placed directly across from the cuttlefish within the holding pen. Animals
319 were scored based on three metrics: 1) time to attack, 2) number of attacks, and 3)
320 duration of attack. These three metrics were combined into a single score. As with the
321 camouflage experiment, scores were compared between treatment and control groups

322 after antibiotic administration, and within treatment and control groups before and after
323 antibiotic administration (e.g. treatment before vs. treatment after antibiotic
324 administration) using the Student's t-test.

325

326 4.2 Sampling

327

328 After the completion of all behavioral assays (pre- and post-antibiotic treatment),
329 each animal was euthanized via immersion into a 10% dilution of ethanol in saltwater.
330 The animals were then dissected under sterile conditions to obtain samples for microbial
331 analyses. The gastrointestinal tract was dissected into four components: esophagus,
332 stomach, cecum, and intestine. A portion of gill tissue was sampled as well. All tissues
333 were stored in separate tubes and flash-frozen in liquid nitrogen. At the end of the
334 experimental period, a 1L water sample was taken from each water table and filtered
335 using a 0.22 micron Sterivex filter for DNA extraction. Lastly, grass shrimp used as the
336 food source throughout the duration of the experiment were collected into 1.8ml sterile
337 cryotubes and frozen for DNA extraction.

338

339 4.3 DNA extraction, sequencing, and 16S rRNA gene statistical analyses

340

341 DNA extractions were performed on gut, tongue, and skin samples using the
342 MoBio PowerSoil 96 Well Soil DNA Isolation Kit (Catalog No. 12955-4, MoBio,
343 Carlsbad, CA, USA). We used the standard 515f and 806r primers (49-51) to amplify
344 the V4 region of the 16S rRNA gene, using mitochondrial blockers to reduce

345 amplification of host mitochondrial DNA. Sequencing was performed using paired-end
346 150 base reads on an Illumina HiSeq sequencing platform. Following standard
347 demultiplexing and quality filtering using the Quantative Insights Into Microbial Ecology
348 pipeline (QIIME2) (52) and vsearch8.1 (53), ASVs were identified using the Deblur
349 method (19) and taxonomy was assigned using the Greengenes Database (May 2013
350 release; <http://greengenes.lbl.gov>). Libraries containing fewer than 1000 reads were
351 removed from further analyses.

352 Alpha diversity for each organ was measured using the Shannon index, as well as
353 by measuring species richness based on actual observed diversity. Significance of
354 differing mean values for each diversity calculation was determined using the Kruskal-
355 Wallis rank sum test, followed by a post-hoc Dunn test with bonferroni corrected *p*-
356 values. Three measures of beta diversity (unweighted UniFrac, weighted UniFrac, and
357 Bray-Curtis) were calculated using relative abundances of each ASV (calculated as ASV
358 read depth over total read depth per library). Significant drivers of community similarity
359 were identified using the ADONIS test with Bonferroni correction for multiple
360 comparisons using the R package Phyloseq (55). Code for microbiome analyses can be
361 found at <http://github.com/hollylutz/CuttlefishMP>. (Authors' note: Sequences and
362 metadata for replication of analyses presented in this study will be uploaded to the Qiita
363 platform and to the European Nucleotide Database upon acceptance for publication.)

364

365 4.4 Sample collection, fixation and sectioning for imaging

366

367 Samples from esophagus, stomach, intestine and cecum of 9 cuttlefish (5 from
368 antibiotic treatment and 4 controls) were dissected and divided in order to include the
369 same individuals in both microscopy and sequencing analyses. Immediately after
370 dividing, samples were fixed with 2% paraformaldehyde in 10 mM Tris pH 7.5 for 12 h
371 at 4 °C, washed in PBS, dehydrated through an ethanol series from 30 to 100%, and
372 stored at -20 °C. Samples were dehydrated with acetone for 1 h, infiltrated with
373 Technovit 8100 glycol methacrylate (EMSdiasium.com) infiltration solution 3 x 1 hour or
374 longer followed by a final infiltration overnight under vacuum, transferred to Technovit
375 8100 embedding solution and solidified for 12 h at 4 °C. Blocks were sectioned to 5 µm
376 thickness and applied to Ultrastick slides (Thermo Scientific). Sections were stored at
377 room temperature until FISH was performed.

378

379 4.5 Fluorescence *in situ* hybridization (FISH)

380

381 Hybridization solution [900 mM NaCl, 20 mM Tris, pH 7.5, 0.01% SDS, 20%
382 (vol/vol) formamide, each probe at a final concentration of 2 µM] was applied to sections
383 and incubated at 46 °C for 2 h in a chamber humidified with 20% (vol/vol) formamide.
384 Slides were washed in wash buffer (215 mM NaCl, 20 mM Tris, pH 7.5, 5mM EDTA) at
385 48 °C for 15 min. Samples were incubated with wheat germ agglutinin (20 µg ml⁻¹)
386 conjugated with Alexa Fluor 488 and DAPI (1 µg ml⁻¹) at room temperature for 30
387 minutes after FISH hybridization to label mucus and host nuclei, respectively. Slides
388 were dipped in distilled cold water, air dried, mounted in ProLong Gold antifade reagent

389 (Invitrogen) with a 1.5 coverslip, and cured overnight in the dark at room temperature
390 before imaging. Probes used in this study are listed in table 2.

391

392 4.6 Image acquisition and linear unmixing

393

394 Spectral images were acquired using a Carl Zeiss LSM 780 confocal microscope
395 with a Plan-Apochromat 40X, 1.4 N.A. objective. Images were captured using
396 simultaneous excitation with 405, 488, 561, and 633 nm laser lines. Linear unmixing was
397 performed using the Zeiss ZEN Black software (Carl Zeiss) using reference spectra
398 acquired from cultured cells hybridized and imaged as above with Eub338 probe labeled
399 with the appropriate fluorophore. Unmixed images were assembled and false-colored
400 using FIJI software (Schindelin *et al.*, 2012).

401

402 FIGURE LEGENDS

403

404 **Figure 1. A single *Vibrio* taxon dominates the esophagus, and a single**
405 ***Piscirickettsiaceae* taxon dominates the gills of the European common cuttlefish in**
406 **captivity**

407 Relative abundance of dominant ASVs (ASVs with >20% maximum relative abundance
408 among samples), colored by ASV, arranged by experimental group (control or treatment),
409 and faceted by organ. Penaid shrimp and sea water from experimental holding tanks are
410 also shown. ASVs are labeled according to the finest level of taxonomic resolution
411 provided by the GreenGenes database. Bars correspond to individual libraries, showing

412 only libraries with >1000 reads. Pictured in the lower right-hand corner is a *S. officinalis*
413 exhibiting camouflage on neutral background.

414

415 **Figure 2. Cuttlefish microbiota show negligible response to antibiotic treatment**

416 (A) Shannon Index and (B) Observed ASV richness of organ microbiota, with and
417 without enrofloxacin treatment. PCoA of (C) weighted UniFrac dissimilarity, (D)
418 unweighted UniFrac dissimilarity, and (E) Bray-Curtis dissimilarity of organ microbiota,
419 with and without enrofloxacin treatment. Points represent individual 16s sequence
420 libraries, with colors corresponding to experimental group (control, treatment), and
421 shapes corresponding to organ (esophagus, stomach, cecum, intestine, and gills).

422

423 **Figure 3. Spatial organization of bacteria in the esophagus of *S. officinalis*.** The

424 image shown is a cross-section of esophagus that was embedded in methacrylate,
425 sectioned, and subjected to fluorescence *in situ* hybridization. (A) Bacteria (magenta)
426 lining the interior of the esophagus in association with the mucus layer (wheat germ
427 agglutinin staining, green). (B) and (C) are enlarged images of the regions marked with
428 arrowheads in (A) where bacteria extend past the edge of the mucus layer. Blue: Host
429 nuclei. Scale bar =100 μm in (A) and 20 μm in (B) and (C).

430

431 **Figure 4. Fluorescence *in situ* hybridization identifies bacteria in the esophagus of**

432 *S. officinalis* as Vibrionaceae. A methacrylate-embedded section was hybridized with a
433 nested probe set containing probes for most bacteria, Gammaproteobacteria,
434 Alphaproteobacteria, and Vibrionaceae. (A) near-universal probe showing a similar

435 bacterial distribution as in figure 3. (B, C, D) Enlarged images of the region marked by
436 the dashed square in (A) showing hybridization with near-universal, Vibrionaceae, and
437 Gammaproteobacteria probes, respectively. (E) Merged image of B, C, and D showing an
438 exact match of the signal from those three probes. (F) Alphaproteobacteria probe
439 showing no hybridization. (G) An independent hybridization with the non-target probe
440 set as a control; no signal is observed. (H) enlarged image of the dashed square in (G).
441 Scale bar=20 μm (A, G); 5 μm (B-F, H).

442

443 **Figure 5. Fluorescence *in situ* hybridization in intestine of *S. officinalis*.** A
444 methacrylate-embedded section was hybridized with the near-universal probe and stained
445 with fluorophore-labeled wheat germ agglutinin to visualize mucus. (A) Bacteria
446 (magenta) are sparsely distributed through the lumen. (B) enlarged image of the dashed
447 square in (A). (C) An independent FISH control with a non-target probe (Hhaem1007);
448 no signal was detected. Scale bar= 20 μm (A, C); 5 μm (B).

449

450 **Figure 6. Fluorescence *in situ* hybridization in spiral cecum of *S. officinalis*.** (A)
451 Bacteria are observed in low abundance in the lumen of spiral cecum. (B) Enlarged
452 image of dashed square in (A). Scale bar=20 μm (A); 5 μm (B).

453

454 **Figure 7. Fluorescence *in situ* hybridization in gills of *S. officinalis*.** Bacteria are
455 observed in small clusters. (A) Overview image. (B, C): enlarged images of the dashed
456 square in (A) showing hybridization with near-universal, and Gammaproteobacteria
457 probes, respectively. (D) Merged image of (B), and (C) showing an exact match of the

458 signal from those two probes. Display in (B, C, and D) was adjusted for clarity. Scale
459 bar=20 μm (A); 5 μm (B-D).

460

461

462

463 ACKNOWLEDGEMENTS

464 We thank Alan Kuzirian, Louie Kerr, Neil Gottel, Wyatt Arnold, Madeline Kim, Elle
465 Hill, Tyler He, and Eric Edsinger. TR and JMW were supported by NSF 1650141. RH
466 thanks the Sholley Foundation for partial support. Amber Durand was supported by the
467 Woods Hole Partnership Education Program. The funders had no role in study design,
468 data collection and interpretation, or the decision to submit the work for publication.

469

470 REFERENCES

471

- 472 1. **McFall-Ngai M.** 2014. Divining the essence of symbiosis: insights from the
473 squid-vibrio model. *PLoS Biol* **12**:e1001783.
- 474 2. **Kerwin AH, Nyholm SV.** 2017. Symbiotic bacteria associated with a bobtail
475 squid reproductive system are detectable in the environment, and stable in the
476 host and developing eggs. *Environ Microbiol* **19**:1463-1475.
- 477 3. **Barbieri E, Bruce J. Paster, Deborah Hughes, Ludek Zurek, Duane P.**
478 **Moser, Andreas Teske, and Mitchell L. Sogin** 2001. Phylogenetic
479 characterization of epibiotic bacteria in the accessory nidamental gland and egg

- 480 capsules of the squid *Loligo pealei* (Cephalopoda: Loliginidae). *Environmental*
481 *Microbiology* **3**:151-167.
- 482 4. **Iehata S, Valenzuela F, Riquelme C.** 2016. Evaluation of relationship between
483 Chilean octopus (*Octopus mimus* Gould, 1852) egg health condition and the egg
484 bacterial community. *Aquaculture Research* **47**:649-659.
- 485 5. **Panetta D, Solomon M, Buresch K, Hanlon RT.** Small-scale rearing of
486 cuttlefish (*Sepia officinalis*) for research purposes. *Marine and Freshwater*
487 *Behaviour and Physiology* **50**:115-124.
- 488 6. **Messenger JB.** 2001. Cephalopod chromatophores: neurobiology and natural
489 history. *Biological Review* **76**:473-528.
- 490 7. **Darmaillacq AS, Dickel L, Mather J.** 2014. *Cephalopod cognition*. Cambridge
491 University Press, Cambridge, UK.
- 492 8. **Hanlon RT, Messenger JB.** 1988. Adaptive coloration in young cuttlefish (*Sepia*
493 *officinalis* L): the morphology and development of body patterns and their relation
494 to behaviour. *Phil Trans R Soc B* **320**:437-487.
- 495 9. **Buresch KC, Ulmer KM, Akkaynak D, Allen JJ, Mäthger LM, Nakamura**
496 **M, Hanlon RT.** 2015. Cuttlefish adjust body pattern intensity with respect to
497 substrate intensity to aid camouflage, but do not camouflage in extremely low
498 light. *Journal of Experimental Marine Biology and Ecology* **462**:121-126.
- 499 10. **Yu C, Li Y, Zhang X, Huang X, Malyarchuk V, Wang S, Shi Y, Gao L, Su Y,**
500 **Zhang Y, Xu H, Hanlon RT, Huang Y, Rogers JA.** 2014. Adaptive
501 optoelectronic camouflage systems with designs inspired by cephalopod skins.
502 *Proc Natl Acad Sci U S A* **111**:12998-13003.

- 503 11. **Chiao CC, Chubb C, Hanlon RT.** 2015. A review of visual perception
504 mechanisms that regulate rapid adaptive camouflage in cuttlefish. *Journal of*
505 *Comparative Physiology A: Neuroethology, Sensory, Neural, and Behavioral*
506 *Physiology* **201**:933-945.
- 507 12. **Tonkins BM, Tyers AM, Cooke GM.** 2015. Cuttlefish in captivity: An
508 investigation into housing and husbandry for improving welfare. *Applied Animal*
509 *Behaviour Science* **168**:77-83.
- 510 13. **Carabotti M, Scirocco A, Maselli MA, Severi C.** 2015. The gut-brain axis:
511 interactions between enteric microbiota, central and enteric nervous systems.
512 *Annals of Gastroenterology* **28**:203-209.
- 513 14. **Koch EJ, Miyashiro T, McFall-Ngai MJ, Ruby EG.** 2014. Features governing
514 symbiont persistence in the squid-vibrio association. *Molecular Ecology* **23**:1624-
515 1634.
- 516 15. **Bloodgood RA.** 1977. The squid accessory nidamental gland: ultrastructure and
517 association with bacteria. *Tissue & Cell* **9**:197-208.
- 518 16. **Pichon D, Isabelle Domart-Coulon, and Renata Boucher-Rodoni** 2017.
519 Cephalopod bacterial associations: characterization and isolation of the symbiotic
520 complex in the Accessory Nidamental Glands. *Boll Malacol* **43**:96-102.
- 521 17. **Collins AJ, LaBarre BA, Won BS, Shah MV, Heng S, Choudhury MH,**
522 **Haydar SA, Santiago J, Nyholm SV.** 2012. Diversity and partitioning of
523 bacterial populations within the accessory nidamental gland of the squid
524 *Euprymna scolopes*. *Appl Environ Microbiol* **78**:4200-4208.

- 525 18. **Gromek SM, Andrea M. Suria, Matthew S. Fullmer, Jillian L. Garcia,**
526 **Johann Peter Gogarten, Spencer V. Nyholm, and Marcy J. Balunas.** 2016.
527 Leisingera sp. JC12, a Bacterial Isolate from Hawaiian Bobtail Squid Eggs,
528 Produces Indigoidine and Differentially Inhibits Vibrios. *Frontiers in*
529 *Microbiology* **7**:1342.
- 530 19. **Lum-Kong A, Hastings TS.** 1992. The accessory nidamental glands of *Loligo*
531 *forbesi* (Cephalopoda: Loliginidae): characterization of symbiotic bacteria and
532 preliminary experiments to investigate factors controlling sexual maturation. . *J*
533 *Zool, Lond* **228**:395-403.
- 534 20. **Tarnecki AM, Burgos FA, Ray CL, Arias CR.** 2017. Fish intestinal
535 microbiome: diversity and symbiosis unravelled by metagenomics. *J Appl*
536 *Microbiol* doi:10.1111/jam.13415.
- 537 21. **Egerton S, Sarah Culloty, Jason Whooley, Catherine Stanton, and R. Paul**
538 **Ross** 2018. The Gut Microbiota of marine fish. *Microbiology* **9**:837.
- 539 22. **Roura A, Doyle SR, Nande M, Strugnell JM.** 2017. You Are What You Eat: A
540 Genomic Analysis of the Gut Microbiome of Captive and Wild *Octopus vulgaris*
541 Paralarvae and Their Zooplankton Prey. *Front Physiol* **8**:362.
- 542 23. **Hanlon RT, Forsythe JW.** 1990. 1. Diseases of Mollusca: Cephalopoda. 1.1.
543 Diseases caused by microorganisms and 1.3 Structural abnormalities and
544 neoplasia., p 23-46 and 203-204. *In* Kinne O (ed), *Diseases of Marine Animals*,
545 vol III. Biologische Anstalt Helgoland, Hamburg.
- 546 24. **Forsythe JW, Hanlon RT, Lee PG.** 1990. A formulary for treating cephalopod
547 mollusc diseases. San Diego: Academic Press.

- 548 25. **Ford LA, Alexander SK, Cooper KM, Hanlon RT.** 1986. Bacterial populations
549 of normal and ulcerated mantle tissue of the squid, *Lolliguncula brevis*. *Journal of*
550 *Invertebrate Pathology* **48**:13-26.
- 551 26. **Takemura AF, Chien DM, Polz MF.** 2014. Associations and dynamics of
552 *Vibrionaceae* in the environment, from the genus to the population level. *Front*
553 *Microbiol* **5**:38.
- 554 27. **Pruzzo C, Huq A, Colwell RR, Donelli G.** 2005. Pathogenic *Vibrio* Species in
555 the Marine and Estuarine Environment, p 217-252. *In* Belkin S, Colwell RR (ed),
556 *Oceans and Health: Pathogens in the Marine Environment* doi:10.1007/0-387-
557 23709-7_9. Springer US, Boston, MA.
- 558 28. **Labella AM, Arahal DR, Castro D, Lemos ML, Borrego JJ.** 2017. Revisiting
559 the genus *Photobacterium*: taxonomy, ecology and pathogenesis. *Int Microbiol*
560 **20**:1-10.
- 561 29. **Mauel MJ, S.J. Giovannoni, and J.L. Fryer** 1999. Phylogenetic analysis of
562 *Piscirickettsia salmonis* by 16S, internal transcribed spacer (ITS) and 23S
563 ribosomal DNA sequencing. *Diseases of Aquatic Organisms* **35**:115-123.
- 564 30. **Azevedo C, Villalba A.** Extracellular Giant Rickettsiae Associated with Bacteria
565 in the Gill of *Crassostrea gigas* (Mollusca, Bivalvia). *Journal of Invertebrate*
566 *Pathology* **58**:75-81.
- 567 31. **Wen C-M, Guang-Hsiung Kou, and Shiu-Nan Chen** 1994. Rickettsiaceae-like
568 Microorganisms in the Gill and Digestive Gland of the Hard Clam, *Meretrix*
569 *lusoria* Röding. *Journal of Invertebrate Pathology* **64**:138-142.

- 570 32. **Moisander P, Andrew D. Sexton, and Meaghan C. Daley.** 2014. Stable
571 Associations Masked by Temporal Variability in the Marine Copepod
572 Microbiome. . PLoS ONE **10**:e0138967.
- 573 33. **Lu X, Sun S, Hollibaugh JT, Mou X.** 2015. Identification of polyamine-
574 responsive bacterioplankton taxa in South Atlantic Bight. Environ Microbiol Rep
575 **7**:831-838.
- 576 34. **Wang K, Zhang D, Xiong J, Chen X, Zheng J, Hu C, Yang Y, Zhu J.** 2015.
577 Response of bacterioplankton communities to cadmium exposure in coastal water
578 microcosms with high temporal variability. Appl Environ Microbiol **81**:231-240.
- 579 35. **Hamdan LJ, Salerno JL, Reed A, Joye SB, Damour M.** 2018. The impact of
580 the Deepwater Horizon blowout on historic shipwreck-associated sediment
581 microbiomes in the northern Gulf of Mexico. Sci Rep **8**:9057.
- 582 36. **Kamalanathan M, Xu C, Schwehr K, Bretherton L, Beaver M, Doyle SM,**
583 **Genzer J, Hillhouse J, Sylvan JB, Santschi P, Quigg A.** 2018. Extracellular
584 Enzyme Activity Profile in a Chemically Enhanced Water Accommodated
585 Fraction of Surrogate Oil: Toward Understanding Microbial Activities After the
586 Deepwater Horizon Oil Spill. Front Microbiol **9**:798.
- 587 37. **Lofthus S, Netzer R, Lewin AS, Heggset TMB, Haugen T, Brakstad OG.**
588 2018. Biodegradation of n-alkanes on oil-seawater interfaces at different
589 temperatures and microbial communities associated with the degradation.
590 Biodegradation **29**:141-157.
- 591 38. **Ribicic D, McFarlin KM, Netzer R, Brakstad OG, Winkler A, Throne-Holst**
592 **M, Storseth TR.** 2018. Oil type and temperature dependent biodegradation

- 593 dynamics - Combining chemical and microbial community data through
594 multivariate analysis. *BMC Microbiol* **18**:83.
- 595 39. **Wang B, Liu H, Tang H, Hu X.** 2018. Microbial ecological associations in the
596 surface sediments of Bohai Strait. *Journal of Oceanology and Limnology* **36**:795-
597 804.
- 598 40. **Allen JJ, Mathger LM, Barbosa A, Buresch KC, Sogin E, Schwartz J, Chubb**
599 **C, Hanlon RT.** 2010. Cuttlefish dynamic camouflage: responses to substrate
600 choice and integration of multiple visual cues. *Proc Biol Sci* **277**:1031-1039.
- 601 41. **Mathger LM, Barbosa A, Miner S, Hanlon RT.** 2006. Color blindness and
602 contrast perception in cuttlefish (*Sepia officinalis*) determined by a visual
603 sensorimotor assay. *Vision Res* **46**:1746-1753.
- 604 42. **Amann RI, Ludwig, W., Schleiffer, K.** 1995. Phylogenetic identification and in
605 situ detection of individual microbial cells without cultivation. *Microbiological*
606 *Reviews* **59**:143-169.
- 607 43. **Neef A.** 1997. Anwendung der in situ-Einzelzell- Identifizierung von Bakterien
608 zur Populations analyse in komplexen mikrobiellen BiozönosenUniversity of
609 Munich.
- 610 44. **Manz W, Amann R, Ludwig W, Wagner M, Schleifer KH.** 1992. Phylogenetic
611 oligodeoxynucleotide probes for the major subclasses of Proteobacteria: problems
612 and solutions. *Systematic and Applied Microbiology* **15**:593-600.
- 613 45. **Chalmers NI, Palmer RJ, Jr., Cisar JO, Kolenbrander PE.** 2008.
614 Characterization of a *Streptococcus* sp.-*Veillonella* sp. community
615 micromanipulated from dental plaque. *J Bacteriol* **190**:8145-8154.

- 616 46. **Valm A. M. MW, J. L., Rieken, C. W., Hasegawa, Y., Sogin, M. L.,**
617 **Oldenbourg, R., Dewhirst, F. E., Borisy, G. G. .** 2011. Systems-level analysis
618 of microbial community organization through combinatorial labeling and spectral
619 imaging. . Proc Natl Acad Sci U S A **108**:4152-4157.

Table 1. Relative abundance dominant ASVs in the esophagus (ASV1, *Vibrio* sp.) and gills (ASV2, Piscirickettsiaceae), both in the class Gammaproteobacteria. T-test of change in relative abundance between treatment and control groups reveals varying degrees of microbial "knockdown" in the treatment groups. * indicates organs in which relative abundance differed significantly between treatment and control animals.

Organ	ASV	Bacterial Family	Genus	Group	Relative Abundance			p-value	df	t
					avg	sd	sem			
Gills*	ASV 2	Piscirickettsiaceae	Unknown	Control	0.969	0.025	0.009	0.01	13.8	2.82
				Treatment	0.824	0.190	0.051			
Esophagus	ASV 1	Vibrionaceae	<i>Vibrio</i> sp.	Control	0.995	0.012	0.004	0.09	14.7	1.83
				Treatment	0.944	0.108	0.028			
Stomach	ASV 1	Vibrionaceae	<i>Vibrio</i> sp.	Control	0.431	0.373	0.141	0.17	10	1.48
				Treatment	0.191	0.309	0.080			
Cecum*	ASV 1	Vibrionaceae	<i>Vibrio</i> sp.	Control	0.437	0.234	0.083	0.002	8.3	4.31
				Treatment	0.064	0.087	0.025			
Intestine*	ASV 1	Vibrionaceae	<i>Vibrio</i> sp.	Control	0.568	0.158	0.056	1.99E-05	8.1	8.81
				Treatment	0.055	0.059	0.016			

620

621

622

623

624

625

626

627

628

629

630

631

632

633

634

635

636

Table 2. FISH probes used in this study

Probe Set	Probe name	Fluorophore(s)	Target organism	Sequence 5' – 3'	Target position	Reference
Experimental	Eub338-I	Alexa 555 or Rhodamine Red X	Most Bacteria	GCTGCCTCCCGT AGGAGT	16S, 338-355	Amann et al. 1990 (42)
	Vib1749	Texas Red X	Vibrionaceae family	AGCCACCTGGTA TCTGCGACT	23S, 1749-1769	Schlundt et al., in prep
	Vib2300	Texas Red X	Vibrionaceae family	TAACTCACGAT GTCCAACCGTG	23S, 2299-2321	Schlundt et al., in prep
	Alf968	Atto 620 or Dy490	Alphaproteobacteria	GGTAAGGTTCT GCGCGTT	16S, 968-985	Neef, A., 1997 (43)
	Gam42a	Atto 647N or Cy5	Gammaaproteobacteria	GCCTTCCCACAT CGTTT	23S, 1027-1043	Manz et al. 1992 (44)
Non-target control	Vei488	Alexa 555	<i>Veillonella</i>	CCGTGGCTTTCT ATTCCG	16S, 488-505	Chalmers et al. 2008 (45)
	PorTan34	Texas Red X	<i>Porphyromonas</i> and <i>Tannerella</i>	GTTAAGCCTATC GCTAGC	16S, 34-51	Mark Welch et al., in prep.
	Fus714	Atto 620	<i>Fusobacterium</i>	GGCTTCCCATC GGCATT	16S, 714-731	Valm et al. 2011 (46)
	Lept568	Atto 647N	<i>Leptotrichia</i>	GCCTAGATGCC TTTATG	16S, 568-585	Valm et al. 2011 (46)
	Hhaem1007	Rhodamine Red X	<i>Haemophilus haemolyticus</i>	AGGCACTCCCAT ATCTCTACAG	16S, 1007-1028	Mark Welch et al., in prep.

637

638

Figure 1. A single *Vibrio* taxon dominates the esophagus, and a single *Piscirickettsiaceae* taxon dominates the gills of the European common cuttlefish in captivity. Relative abundance of dominant ASVs (ASVs with >20% maximum relative abundance among samples), colored by ASV, arranged by experimental group (control or treatment), and faceted by organ. Penaid shrimp and sea water from experimental holding tanks are also shown. ASVs are labeled according to the finest level of taxonomic resolution provided by the GreenGenes database. Bars correspond to individual 16s rRNA sequence libraries, showing only libraries with >1000 read depth. *S. officinalis* pictured in the lower right-hand corner.

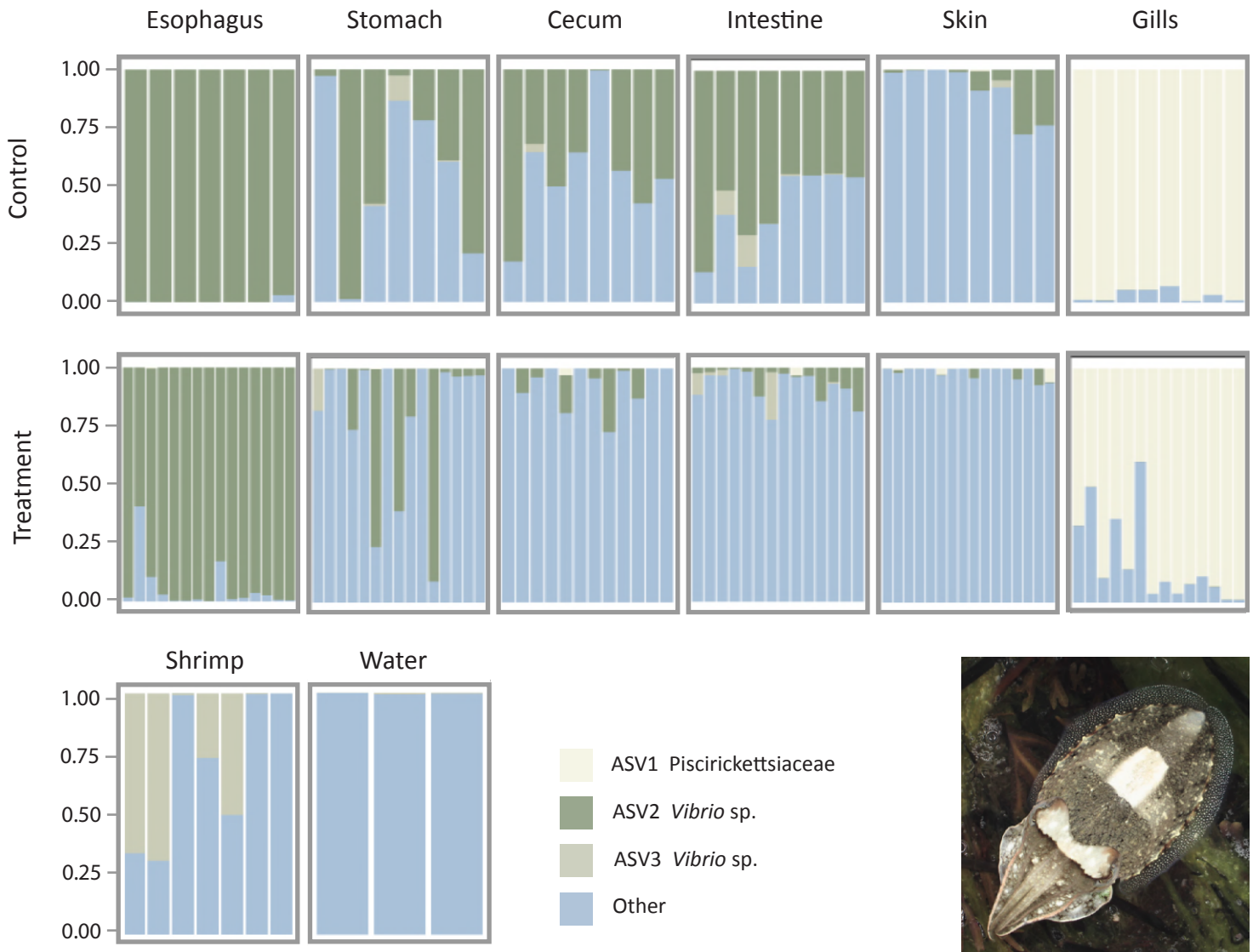


Figure 2. Cuttlefish microbiota show negligible response to antibiotic treatment

(A) Shannon Index and (B) Observed ASV richness of organ microbiota, with and without enrofloxacin treatment. PCoA of (C) unweighted UniFrac dissimilarity, (D) weighted UniFrac dissimilarity, and (E) Bray-Curtis dissimilarity of organ microbiota, with and without enrofloxacin treatment. Points represent individual 16s sequence libraries, with colors corresponding to experimental group (control, treatment), and shapes corresponding to organ (esophagus, stomach, cecum, intestine, and gills).

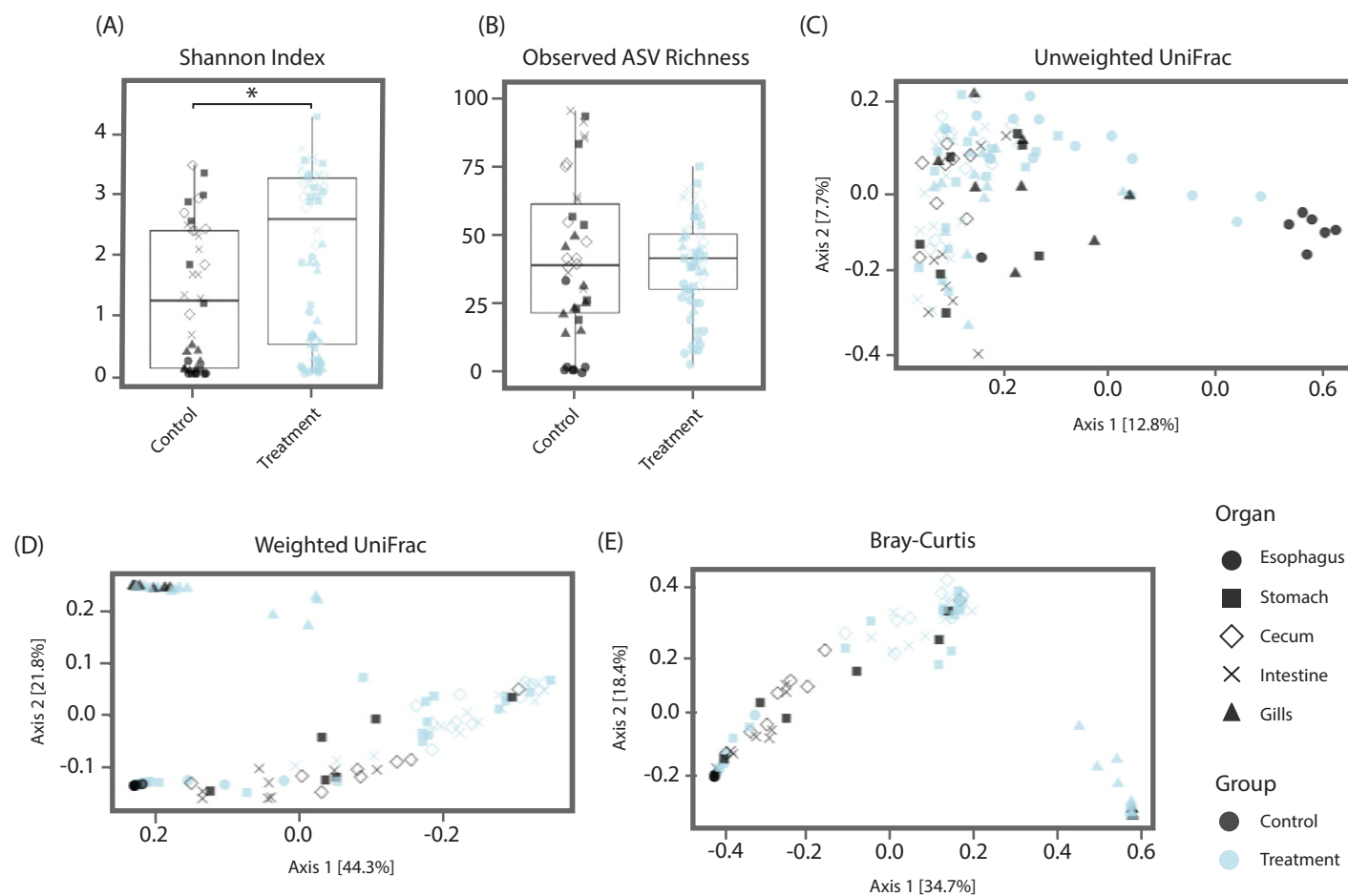


Figure 3. Spatial organization of bacteria in the esophagus of *S. officinalis*. The image shown is a cross-section of esophagus that was embedded in methacrylate, sectioned, and subjected to fluorescence *in situ* hybridization. (A) Bacteria (magenta) lining the interior of the esophagus in association with the mucus layer (wheat germ agglutinin staining, green). (B) and (C) are enlarged images of the regions marked with arrowheads in (A) where bacteria extend past the edge of the mucus layer. Blue: Host nuclei. Scale bar =100 μ m in (A) and 20 μ m in (B) and (C).

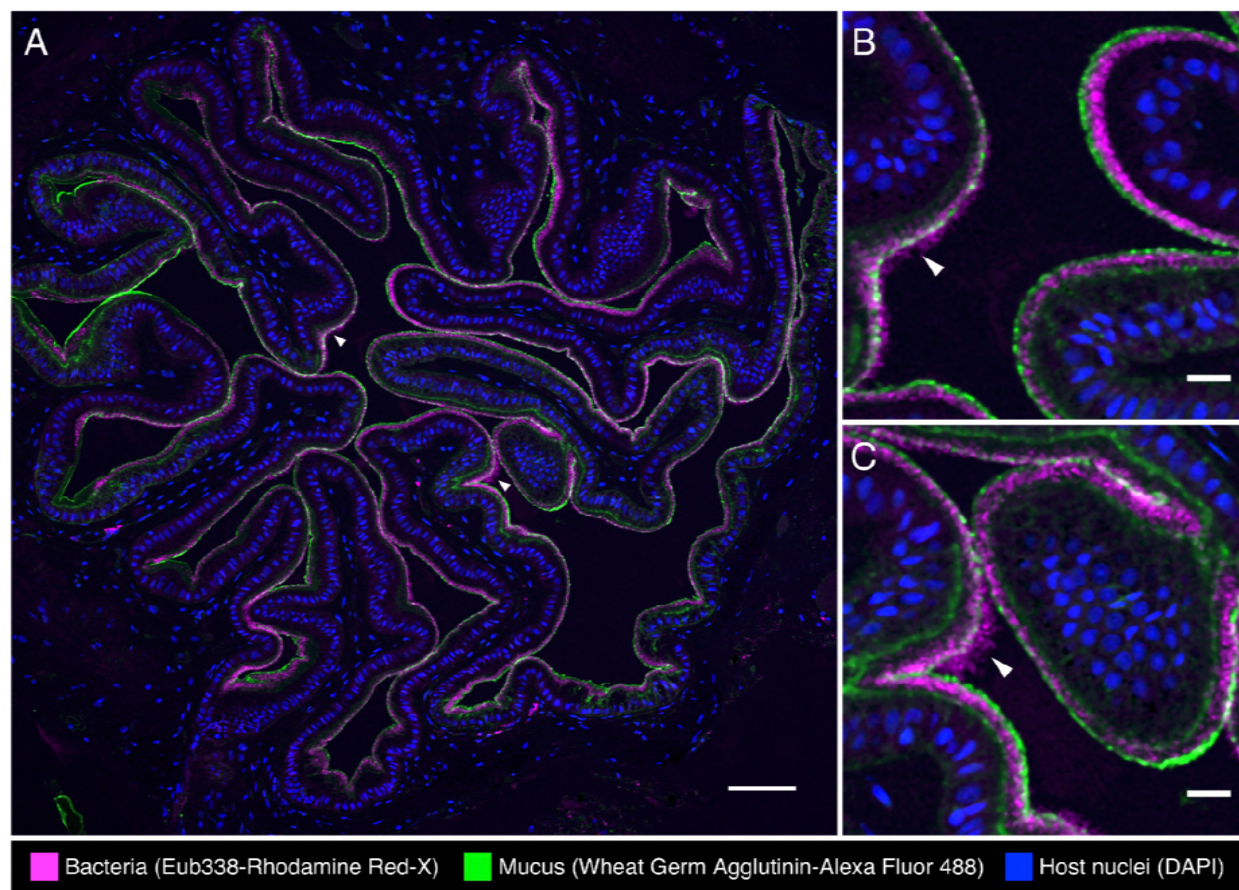
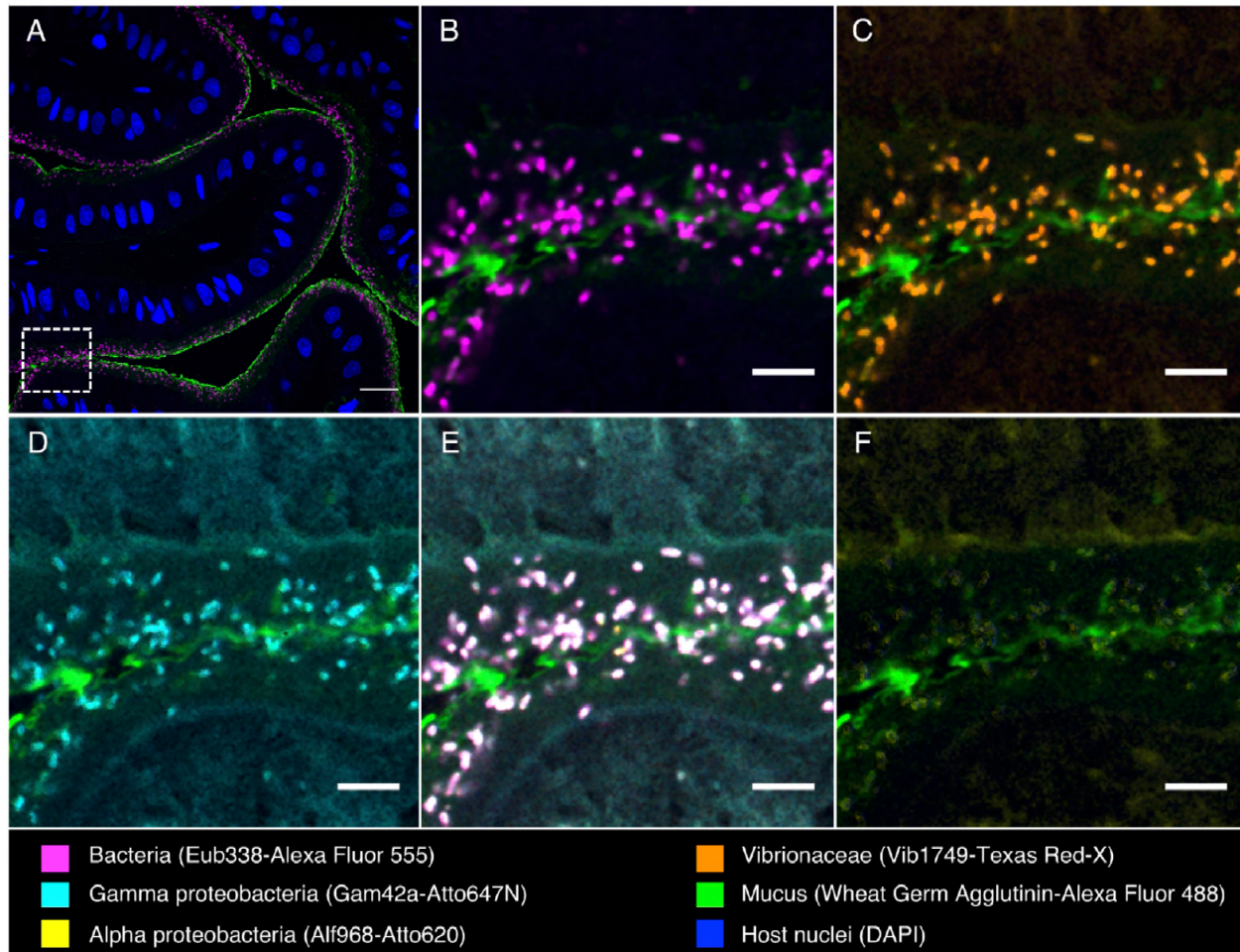


Figure 4. Fluorescence *in situ* hybridization identifies bacteria in the esophagus of *S. officinalis* as Vibrionaceae. A methacrylate-embedded section was hybridized with a nested probe set containing probes for most bacteria, Gammaproteobacteria, Alphaproteobacteria, and Vibrionaceae. (A) Near-universal probe showing a similar bacterial distribution as in figure 3. (B, C, D) Enlarged images of the region marked by the dashed square in (A) showing hybridization with near-universal, Vibrionaceae, and Gammaproteobacteria probes, respectively. (E) Merged image of (B, C, and D) showing an exact match of the signal from those three probes. (F) Alphaproteobacteria probe showing no hybridization. (G) An independent hybridization with the non-target probe set as a control; no signal is observed. (H) enlarged image of the region marked by the dashed square in (G). Scale bar=20 μm (A, G); 5 μm (B-F, H).

Specific probe set



Non-target probe set

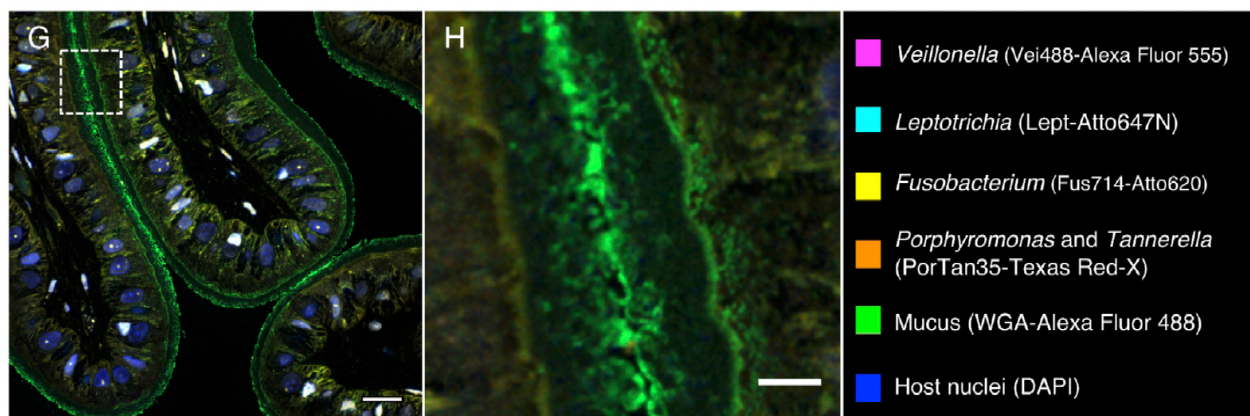


Figure 5. Fluorescence *in situ* hybridization in intestine of *S. officinalis*. A methacrylate-embedded section was hybridized with the near-universal probe and stained with fluorophore-labeled wheat germ agglutinin to visualize mucus (green). (A) Bacteria (magenta) are sparsely distributed through the lumen. (B) enlarged image of the region marked by the dashed square in (A). (C) An independent FISH control with a non-target probe (*Hhaem1007*); no signal was detected. Scale bar= 20 μm (A, C); 5 μm (B).

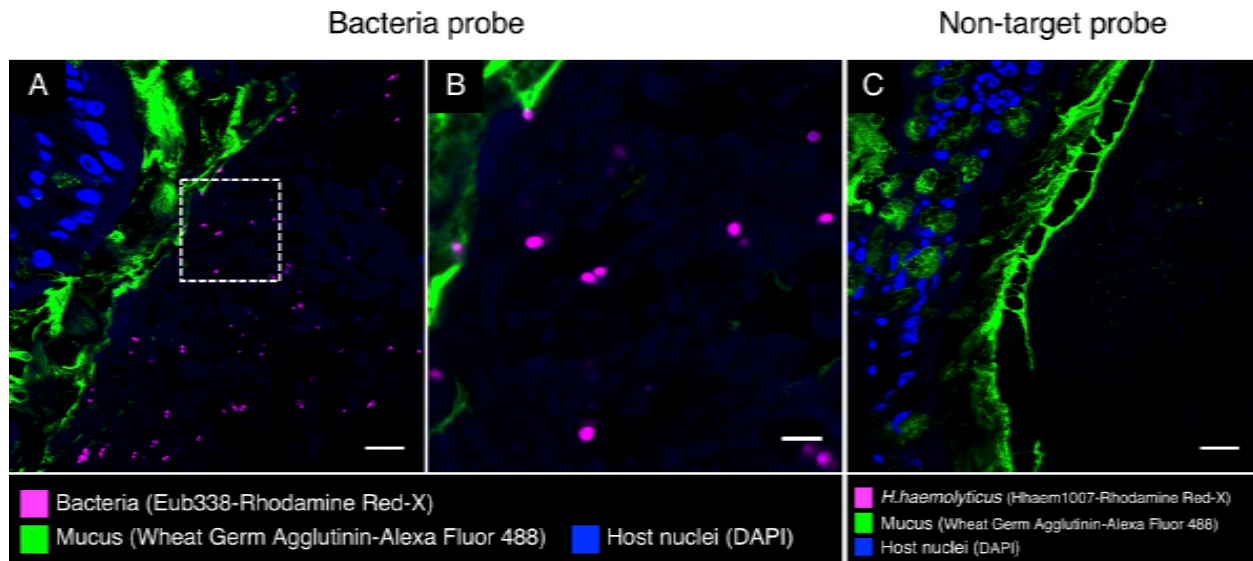


Figure 6. Fluorescence *in situ* hybridization in cecum of *S. officinalis*. A methacrylate-embedded section was hybridized with the near-universal probe and stained with fluorophore-labeled wheat germ agglutinin to visualize mucus (green). (A) Bacteria are observed in low abundance in the lumen of cecum. (B) Enlarged image of region marked by the dashed square in (A). Scale bar=20 μ m (A); 5 μ m (B).

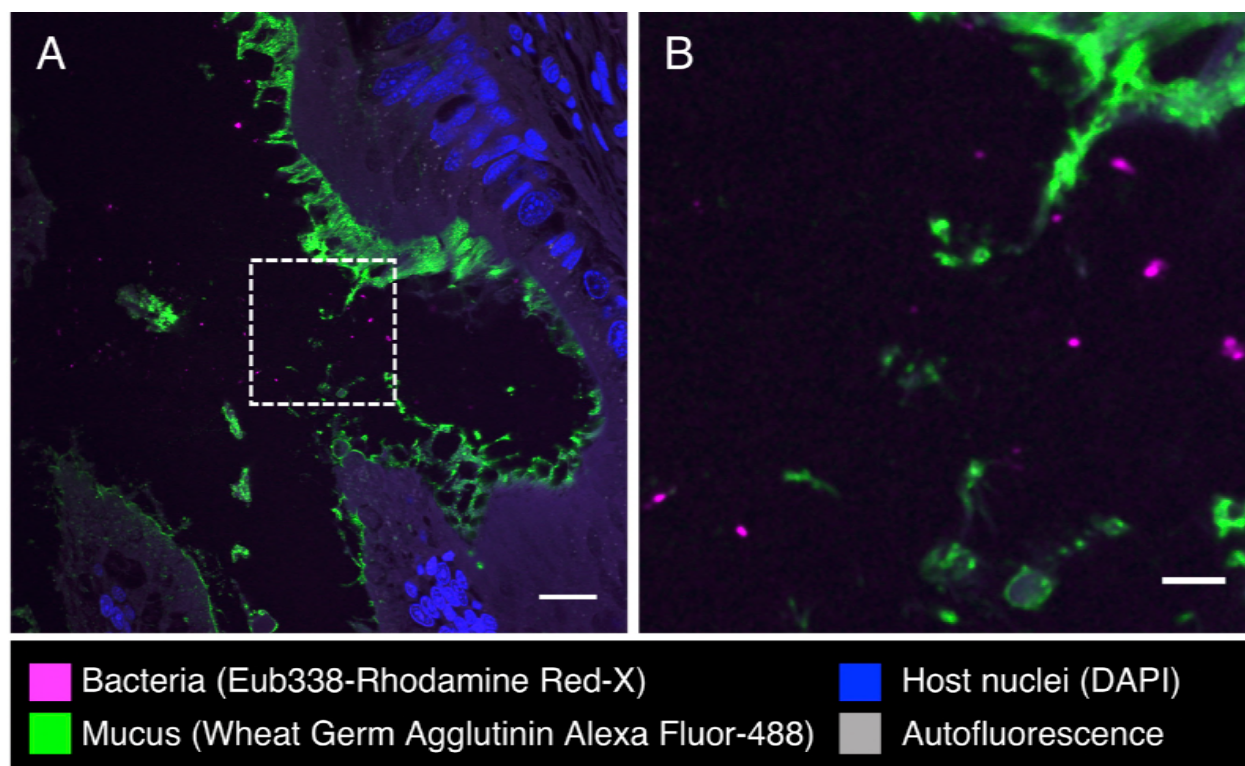


Figure 7. Fluorescence *in situ* hybridization in gills of *S. officinalis*. A methacrylate-embedded section was hybridized with the near-universal probe and stained with fluorophore-labeled wheat germ agglutinin to visualize mucus (green). Bacteria are observed in small clusters. (A) Overview image. (B, C): enlarged images of the region marked by the dashed square in (A) showing hybridization with near-universal, and Gammaproteobacteria probes, respectively. (D) Merged image of (B), and (C) showing an exact match of the signal from those two probes. Display in (B, C, and D) was adjusted for clarity. Scale bar=20 μm (A); 5 μm (B-D).

